JOURNAL OF APPLIED GEOSPATIAL INFORMATION

Vol 7 No 1 2023

http://jurnal.polibatam.ac.id/index.php/JAGI
ISSN Online: 2579-3608

# Faulting Mechanism of Tarutung Earthquake 2022 Mw 5.8 Using Moment Tensor Inversion: A Preliminary Study

Endah P. Sari [1,2], Resa Idha [1,2], Yusran Asnawi [3], Andrean V. H. Simanjuntak [2,4], Syahrul Humaidi [1*], Umar Muksin [4]

[1] Post Graduate Program (Physics), FMIPA, Universitas Sumatera Utara, Medan, Sumatra Utara, Indonesia
[2] Agency of Meteorological Climatology and Geophysical for Indonesia, Medan, Sumatra Utara, Indonesia
[3] Department of Information Technology, Universitas Islam Ar-Raniry, Banda Aceh, Aceh
[4] Tsunami Disaster Mitigation Research Centre (TDMRC), Universitas Syiah Kuala, Banda Aceh, Aceh
Corresponding author's email: syahrul1@usu.ac.id

**Received:** February 17, 2023
**Accepted:** June 27, 2023
**Published:** June 27, 2023



**Abstract**

On October 1, 2022, a modeate earthquake with a magnitude of 5.8 was occurred in the Tarutung and generated by an active fault at a shallow depth of 10 km. In this study, relocating the hypocenter and determining the mechanism of the earthquake was carried out to understand the active tectonic structure. The distribution of hypocenter relocation figures a pull-apart pattern at shallow depths. The earthquake mechanism shows a dextral pattern in the Northwest – Southeast direction with a strike of 138º – 158º. The aftershocks are more dominantly distributed in the pull-apart system in the southeastern part and show the greater part of the transfer of seismic static stress to the southeastern side of the Toru fault. The pull-apart tectonic system scheme in the Tarutung basin with secondary faults as extensional faults is proposed to be a fault source model that forms a negative-flower structure geological pattern. The results of this study can be used as a reference for the Tarutung tectonic system and applied as a mitigation study.

**Keywords:** Earthquake, Hypocenter, Tectonic Mechanism, Tarutung, Momen Tensor

## 1. Introduction

The island of Sumatra is located at the subduction system between the Indo-Australian towards beneath Eurasian tectonic plates (Gahalut et al., 2006; McCafrey, 2008; Sieh and Natawidjaja, 2000). The tectonic activity produces complex tectonic systems such as active subduction zones and active faults as shown in Figure 1. Complex tectonic activities affect seismicity processes in the North Sumatra region. The Meteorology, Climatology and Geophysics Agency for Indonesia (BMKG) records that more than 1,000 earthquakes occur every year in the North Sumatra region and the last one is the damaging earthquake in Tarutung in 2022. On October 1, 2022, the active Sumatran fault generated a significant earthquake that rocked the North Tapanuli region and surrounding. BMKG reported the epicenter coordinates at 2.13 N – 98.89 E that is located around 15 km northwest of North Tapanuli Regency. BMKG updated the parameters from the initial strength of M6.0 to M5.8. The earthquake was felt in the Tarutung, Sipahutar, North Tapanuli, Sibolga, Rantau Prapat, Gunung Sitoli until to the Aceh region including Singkil and Tapaktuan.

Geographically, Tarutung as the capital of North Tapanuli Regency is one of the affected areas closest to the epicenter of the earthquake because it is traversed by the Toru fault (Muksin et al., 2013; Bradley et al., 2017). In addition, the characteristics of the Tatutung earthquake are categorized as type I because it was preceded by a mainshock without a foreshock and followed by a series of aftershocks (Pasari et al., 2021, Simanjuntak and Ansari, 2022). Seismicity studies such as determining hypocenters and earthquake fault mechanisms are very important to provide information on subsurface structures. One of the obstacles in seismicity studies is the uncertainty that the location of the hypocenter is far from the fault line, making it difficult to interpret the geological structure. Therefore, it is necessary to do an accurate relocation to improve the quality of the hypocenter.

In this study, the Double-difference method was used to relocate the Tarutung earthquake series. Several relocation studies have been carried out, such as Lake Toba seismicity relocation (Simanjuntak et al., 2022), Sumatra seismicity statistics (Pasari et al., 2021; Nurana et al., 2020), Central Aceh seismicity

(Muksin et al., 2021, Simanjuntak et al., 2022), Sumatran seismic hazard model (Asnawi et al., 2022; Irwandi et al., 2021) but have not been carried out in the Tarutung area. In addition, the fault mechanism (strike, dip, and rake) was determined to support the hypocenter relocation results. Determination of the fault mechanism uses the principle of simultaneous inversion with a probabilistic approach that can calculate the geometry of the fault as well as improve earthquake parameters. The results of the relocation and the Tarutung earthquake fault model can be a renewable geological reference and consideration in disaster management efforts in the research area.

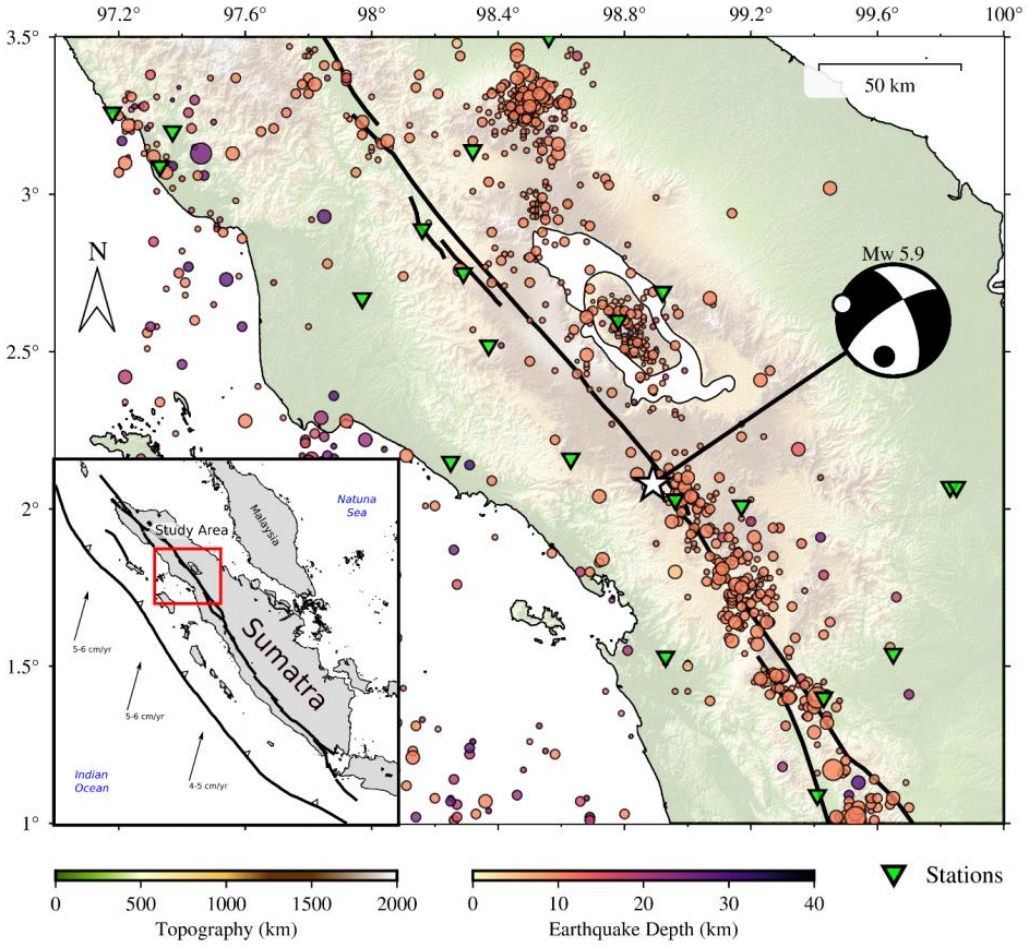


Fig. 1. Seismic map of North Sumatra Province five-year catalog (2017 – 2022) with the Tarutung 2022 Mw 5.8 earthquake (white star with dextral focus mechanism). The black line is the active Sumatran fault while the green triangle is the seismic station of the BMKG network.

## 2. Methodology

### 2.1 Double Difference Relocation

The Double-Difference method is powerful to relocate the earthquake hypocenters into specific clusters by inverting the location parameters. In this method, the main earthquake or event master is not needed. Therefore, this method simultaneously relocate large numbers of earthquakes. The goal of the double-difference algorithm is to minimize the difference in residual travel time for pairs of earthquakes at the same station and solution will be free from travel time errors related to speed variations, although there will still be random errors at the initial location (Waldhauser, 2001). The difference between the difference in observation and calculation travel time from the two earthquake data ($dt_k^{ij}$) on Fig. 2 can be written as the equation (1) below

$$dt_k^{ij} = \left(T_k^i - T_k^j\right)^{obs} - \left(T_k^i - T_k^j\right)^{cal} \quad (1)$$

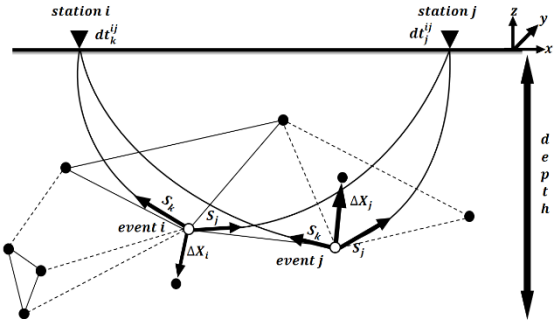


Fig. 1. Illustration of a double-difference algorithm (modified from Waldhauser and Ellsworth, 2000) that depicts black and white circles as the distribution of hypocenters connected by earthquakes with a cross-correlation (solid line) or catalog (dotted line). Earthquakes i and j are recorded at the same stations k and l with the difference in travel time from the positions of the two adjacent earthquakes, so the shape of the raypath (source to station) tends to be the same, which means that it passes through the medium with almost the same slowness.

Equation (1) shows the residual of arrival time ($dt_k^{ij}$) from two earthquakes *i* and *j* in the observations seismic station *k* based on the difference in observation and calculation travel times for the two earthquakes. From Fig. 2, $T_k^i$ is the arrival time of earthquake *i* to the seismic station *k*, while $T_k^j$ is the arrival time of earthquake *j* to the seismic station *k*. If slowness is not constant due to the relationship between travel time and the location of the earthquake is not linear. The hypocenter parameters are represented by x, y, z, and which are the initial position and time. The residual travel time is determined by changes in the 4 parameters for each of the 2 earthquakes involved in the earthquake pair. The distribution of earthquake hypocenters in groups (clusters) generally provides important information regarding the presence of a fault. Hypocenter clusters were obtained by relocation so that good relocation results and small error values were obtained.

Each earthquake has travel time information that is connected to one another and recorded at the same station, so that it can be cross-corrected between times and places. This is meant to measure the degree of similarity of the many earthquakes recorded at one station. This similarity will affect hypocenter clusters after relocation. The algorithm in the HypoDD program uses the least-square inversion method. The hypocenter error in the HypoDD program uses the trial and error method to get the low residual travel time.

### 2.2 Moment tensor inversion

The mechanism of the earthquake source can be described conventionally by analyzing the polarity of the P waves recorded on the seismometer, through trial-error techniques but it is too subjective. A more objective way is to use the moment tensor on the displacement signal. Displacement has a linear relationship to the moment tensor so that it allows for seismic wave inversion. Aki and Richard (2002) stated that the moment tensor is defined by force couples and force dipole which in matrix form can be expressed in equation (2).

$$M = \begin{bmatrix} M_{xx} & M_{xy} & M_{xz} \\ M_{yx} & M_{yy} & M_{yz} \\ M_{zx} & M_{yx} & M_{zz} \end{bmatrix} = \begin{bmatrix} M_{11} & M_{12} & M_{13} \\ M_{21} & M_{22} & M_{23} \\ M_{31} & M_{32} & M_{33} \end{bmatrix} \quad (2)$$

The nine basic components of the moment tensor are represented by a 3x3 matrix. The inversion used is a type of linear inversion which is over determined, where the amount of data is far more than the number of model parameters. The source factor is indicated by the tensor (*m*), the Green function is expressed in the form of a seismogram produced by the source m, while the instrument response is omitted, so that the displacement (*u*) at an observing station on the earth's surface is expressed as equation (3).

$$u_i(t) = \sum_{j=1}^{6} G_{ij}(t) m_j \quad (3)$$

equation (3) can be written in matric as follows.

$$\begin{bmatrix} u_1 \\ u_2 \\ \cdots \\ \cdots \\ u_n \end{bmatrix} = \begin{bmatrix} G_{11} & G_{12} & G_{13} & G_{14} & G_{15} & G_{16} \\ G_{21} & G_{22} & G_{23} & G_{24} & G_{25} & G_{26} \\ G_{31} & G_{23} & G_{33} & G_{34} & G_{35} & G_{36} \\ \cdots & \cdots & \cdots & \cdots & \cdots & \cdots \\ \cdots & \cdots & \cdots & \cdots & \cdots & \cdots \\ G_{n1} & G_{n2} & G_{n3} & G_{n4} & G_{n5} & G_{n6} \end{bmatrix} \begin{bmatrix} m_1 \\ m_2 \\ m_3 \\ m_4 \\ m_5 \\ m_6 \end{bmatrix} \quad (4)$$

$$\mathbf{u = G\,m} \quad (5)$$

Where, u is the amount of data, m is the model parameter, and *G* is the (*NxM*) matrix. The model parameters cannot be obtained directly from matrix *G* inversion because the order of the matrices is not the same (*N*≠*M*) so the solution to the equation becomes as follows.

$$\mathbf{m} = (\mathbf{G}^{\mathrm{T}}\mathbf{G})^{-1}\mathbf{G}^{\mathrm{T}}\mathbf{u} \quad (6)$$

The direction of the fault plane obtained from the moment tensor inversion results requires that all components recorded at each station are inverted. The observed signal will be adjusted to the shape of the synthetic signal by adjusting the frequency domain.

## 3. Results and Discussion

### 3.1 Earthquake Relocation and Cluster

In this study, the 1-Dimensional seismic velocity model from Simanjuntak et al., (2022) is used for the computational process on HypoDD to relocate the earthquake hypocenter. The final relocation is obtained by setting parameters, namely the separation distance between hypocenters is 40 km, the maximum number of earthquakes is 10, the maximum distance between earthquake pairs is 20 km and the hypocenter and centroid are 0 – 80 km. The BMKG catalog hypocenters still form a lot of solutions that are made fixed and trapped at depths of 10 and 33 km so they need to be relocated to make the variation of depth better.

Several earthquakes with small magnitudes were reduced because the total number of observation stations did not meet the criteria. In addition, hypocenters that are too spread out and too weak to be considered a partner will also be reduced. A total of 124 earthquakes were successfully relocated with RMS values as shown in Figure 3. In Figure 3, the distribution of the hypocenters of the earthquakes spread before the HypoDD computation was applied with a fixed depth pattern at a value of 5 km. Changes are seen after the relocation of the HypoDD with distribution that is more concentrated on fault lineaments, although there are still some earthquakes that are outside the fault lines.

Changes in the hypocenter depth value can also be seen clearly on the vertical section. The dominant earthquakes were at depths < 8 km, and the fixed-depth pattern was no longer visible. A priori weighting is given with a weight value <0.5, which means that the observation data is very good and in accordance with the calculations. The delay between the observation and calculation times is close to 0 (similar) and the relocation results can be said to be good. In addition, the relocation results show a very good rms with not too far cluster-centroid distance.

The mechanism of the earthquake source is obtained by matching and inverting the body-wave and surface-wave separately or better known by a device capable of characterizing the mechanism of a strong earthquake source named Grond (Heimann et al., 2018). Surface waves are easier to model synthetically, because surface waves have a large amplitude and long duration, so they are often used in the inversion process of earthquake mechanisms. The Grond device is capable of a lot of seismic event data

in parallel, so it has an accountable level of effectiveness. To get a representative source mechanism, good seismic wave recordings are needed as input data. The waves used are recorded at each station with a distance of 0 – 4° as shown in Figure 4 which is still in speed units. In this inversion process, velocity data from each seismometer sensor must be integral to obtain a displacement signal. The displacement signal is then analyzed by inversion to obtain the appropriate fault model. In addition, the displacement signal is given instrument response correction to obtain the original seismic signal originating from the source. Instrumental correction is provided to avoid seismic signals from several stations that have experienced attenuation and amplification.

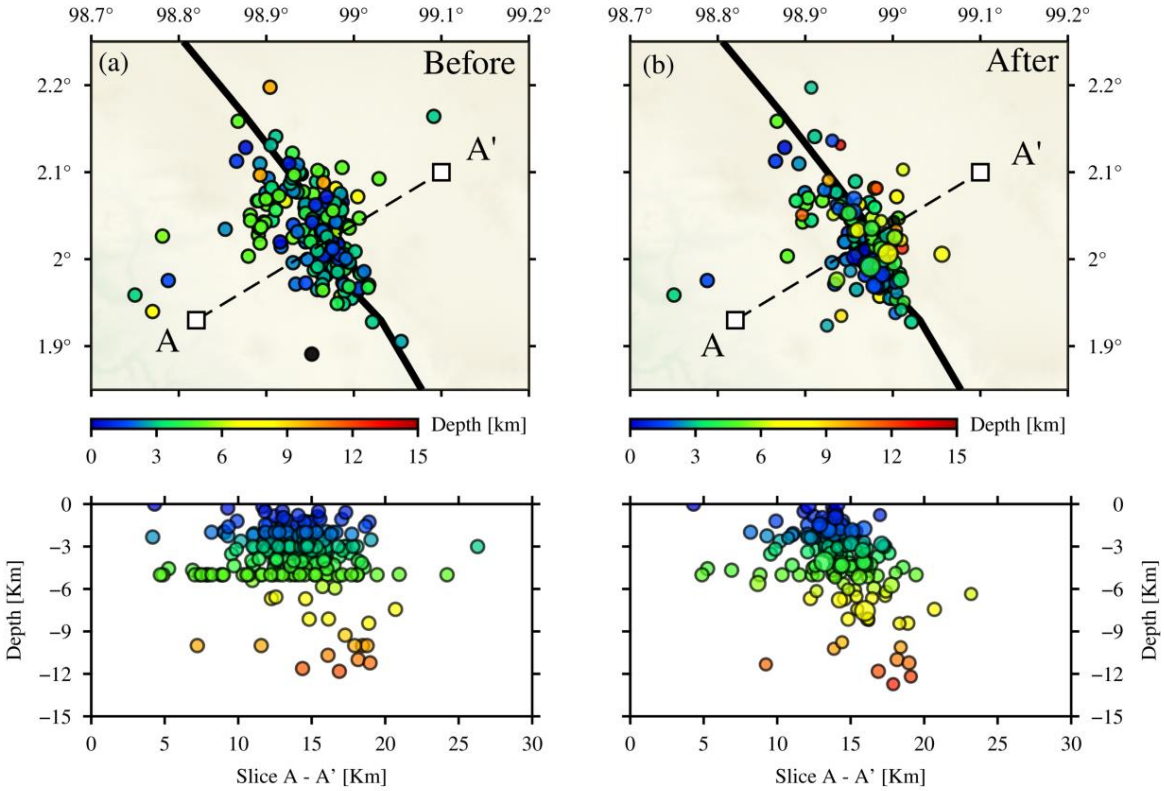


Fig. 3. (upper panle) Map of earthquake distribution shows the comparison between before and after relocation using hypoDD and vertical profile with similar comparison for Tarutung earthquake.

The moment tensor inversion process using a displacement signal is more representative of the earthquake source process as shown in Figure 5. The results of matching the observed (black line) and synthetic (red line) seismic signals in Figure 5 show dominant results similar to the case of the M5.8 earthquake. Surface waves were modeled from 12 (twelve) stations in the M5,8 main earthquake, there were 3 (three) stations namely the MNSI, PABI, PLSI stations which seemed the most compatible with close to 100% match, besides that other stations also had a reliable and consistency match.

The probability density function (PDF) graph showing the depth element of the earthquake source in Figure 5 shows that the highest value is seen at a depth of around 6 – 7 km, which means that earthquakes originate from the shallow crust of the earth, or are usually due to fault activity. This is evidence that the 2022 Tarutung earthquake was generated by the movement of a shallow fault around the North Tapanuli – North Sumatra region. The results of the bootstrap analysis succeeded in updating the hypocenter parameters, in which the location of the main earthquake epicenter shifted ~ 15 km to the southeast, while the depth of the source of the earthquake was ~ 6 km. The seismic moment for the mainshock is 1.2 x $10^{16}$ Nm while 6.4 x $10^{15}$ Nm and 3.2 x $10^{15}$ Nm for M 5.3 dan M 5.1, respectively.

The previous seismic energy and moment releases occurred in 2008 and 2011 with a strike-slip mechanism in the Tarutung area. Long before that, tectonic activity around this area had triggered major earthquakes such as 1921 (Mw 6.6), 1967 (Mw 6.6) and 1980 (Bellier et al., 1997; Muksin et al., 2014; Hurukawa et al., 2014). However, things are different with the condition of the Renun segment which has a seismic gap along the Sumatran fault which extends 220km. This indicates that there is a high fault lock in the upper crust asperity zone.

In recent years BMKG has monitored the swarm phenomenon in the western part of the Renun segment which indicates a contribution from volcanic activity. Seismic activity in the Tarutung area began to be recorded properly from 2008 because many seismic stations on the BMKG network were built at that time, so that prior to that monitoring of small earthquakes was not well recorded. Starting in 2019 the BMKG seismic network will be strengthened so that small and even micro earthquakes with a magnitude > 1.0 can be detected and analyzed properly. This makes it possible to know the subsurface tectonic conditions with greater certainty

based on quite complete historical seismic data. Moreover, source mechanism parameters obtained from the inversion of earthquake signals or waveforms using an earthquake duration of 20 - 50 seconds, namely the direction of the fault line or strike ranges from 138° - 158°, dip 51° - 85° and rake 146° - 172° in the plane nodal 1.

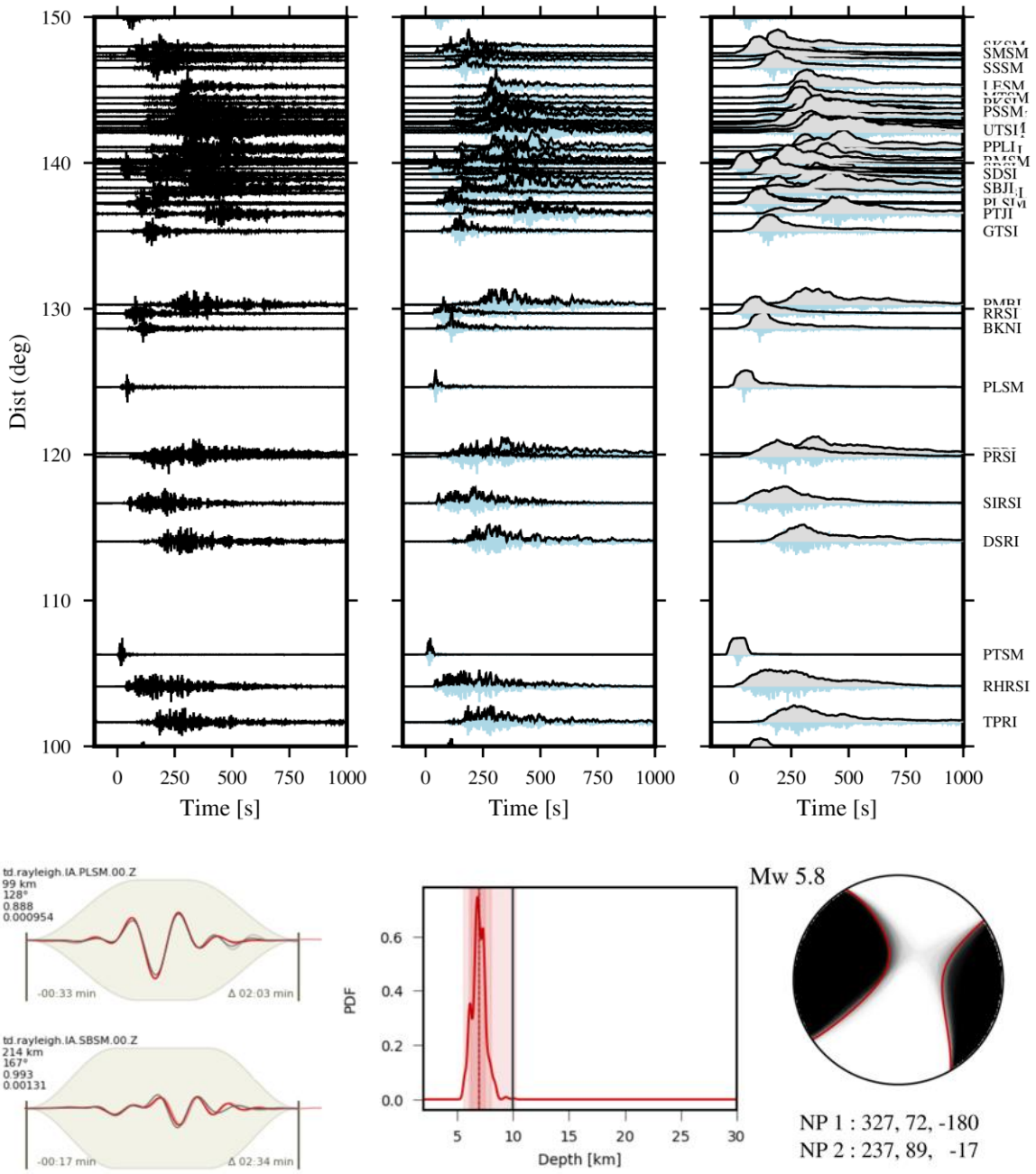


Fig. 4. (Upper panel) Example of a signal recording of one of the earthquakes on the BMKG (IA) station network for the vertical component. On the left, the original recording of the Tarutung earthquake, and the middle part is the envelope result to see the dominant wave amplitude and the right part is the smoothing process to see the time duration of the earthquake. (Bottom panel) Two examples of signal inversion results for the largest event (Main earthquake M5.8) and error values. Earthquake depth changed from 10 km previously to ~6-7km after the inversion. The fracture model obtained is a right (dextral) pattern.

For nodal plane 2, the fault parameters resulting from the inversion are strike between 233° - 250°, dip 57° - 83° and rake 5° - 39°. The largest moment magnitude magnitude scale is Mw 5.8 which occurred during the main earthquake, while the others varied between 4.50 – 5.30 which was a series of aftershocks with a fairly strong category originating at a depth of 6.0 – 10.5 km as shown in Figure 6. The model with data before relocation has a greater number of hypocenters with better rms than data that has not been relocated. Figures 5 (a) and (b) illustrate the distribution of aftershocks (M4.5 – M5.3) concentrated in the zone where the Toru and Renun segments meet. The strike direction shows a uniform pattern, namely the Northwest – Southeast direction according to the Sumatra fault shift.

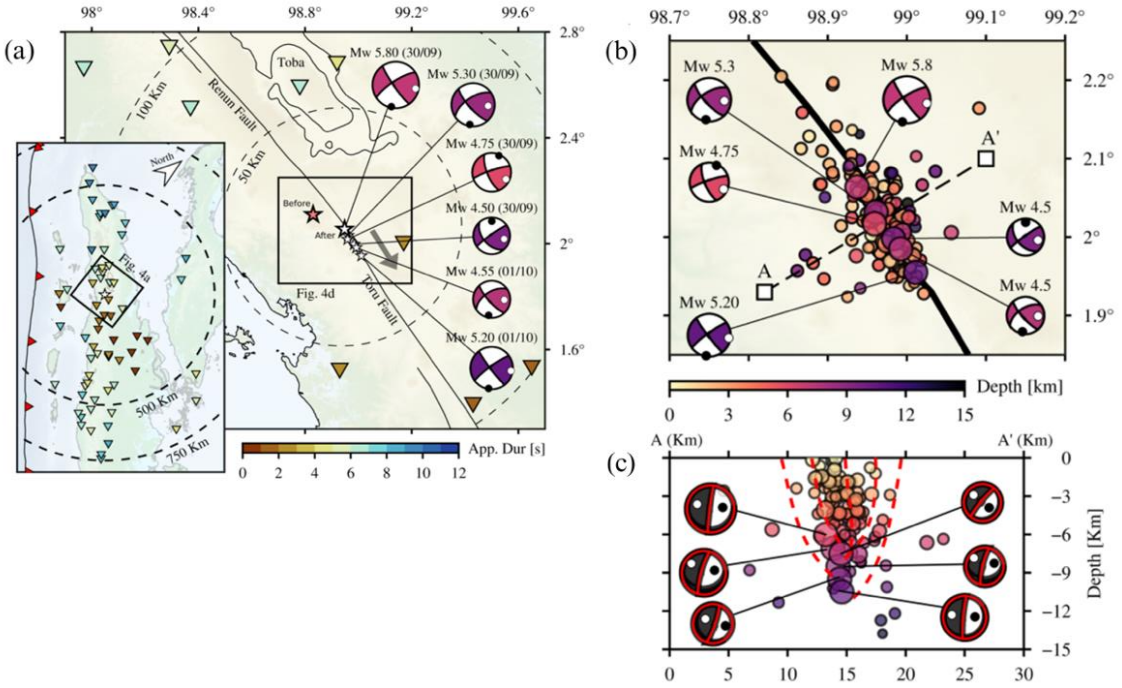


Fig. 5. (a) Solution to the fault mechanism of the selected main earthquake and aftershocks M4.5; (b) Earthquake seismicity and earthquake mechanism solutions in the pull-apart system to the south of the Toru fault segment; (c) The vertical cross section of the distribution A-A' depicts a local system called the negative flower structure which is under a pull-apart system.

From the results obtained, the tectonic system describes a pull-apart basin. In addition, the results of relocation of the hypocenter confirmed the presence of pull-apart. Earthquake clusters and earthquake fault mechanisms form a fault structure in the northwest (NW) – southeast (SE) direction which is located in the extensional zone of the Toru and Renun faults.

## 5. Conclusions

From the results of the research that has been done, some conclusions can be formulated as follows. The hypocenter distribution of the Tarutung Mw 5.8 earthquake series before being relocated with HypoDD has a spreading pattern with a dominant fix-depth depth of 5 km. The localization that was carried out further improved the quality of the distribution of the Tarutung earthquake hypocenter with rms < 0.5 s. The solution to the earthquake source mechanism shows a dextral fault mechanism pattern in the Northwest – Southeast (NW – SE) direction with a strike of 138º – 158º. The aftershocks are more dominantly distributed in the pull-apart system in the southeastern part and show the greater part of the transfer of seismic static stress to the southeastern side of the Toru fault. The pull-apart tectonic system scheme in the Tarutung basin with secondary faults as extensional faults is proposed to be a fault source model that forms a negative-flower structure geological pattern. The results of this study can be used as a reference for studying the Tarutung tectonic system and applied as a mitigation study.

## Acknowledgements

We thank to Badan Meteorologi Klimatologi dan Geofisika (BMKG) for providing the seismic data. We thank the fruitful discussion with Umar Muksin and Andrean Simanjuntak for their guidance to process the seismic data. We thank also for colleagues of BMKG office in the 1st regional in Medan for the survey report after Tarutung earthquake.

## References

Aki, K., & Richards, P. G. (2002). Quantitative seismology.

Asnawi, Y., Simanjuntak, A., Muksin, U., Rizal, S., Syukri, M. S. M., Maisura, M., & Rahmati, R. (2022). Analysis of Microtremor H/V Spectral Ratio and Public Perception for Disaster Mitigation. GEOMATE Journal, 23(97), 123-130.

Asnawi, Y., Simanjuntak, A. V. H., Muksin, U., Okubo, M., Putri, S. I., Rizal, S., & Syukri, M. (2022). Soil classification in a seismically active environment based on join analysis of seismic parameters. Global Journal of Environmental Science and Management, 8(3), 297-314.

Bellier, O., Sebrier, M., Pramumijoyo, S., Beaudouin, T., Harjono, H., Bahar, I., & Forni, D. O. (1997). Paleoseismicity and seismic hazard along the Great Sumatran Fault (Indonesia). Journal of Geodynamics, 24(1-4), 169-183.

Bradley, K. E., Feng, L., Hill, E. M., Natawidjaja, D. H., & Sieh, K. (2017). Implications of the diffuse deformation of the Indian Ocean lithosphere for slip partitioning of oblique plate convergence in Sumatra. Journal of Geophysical Research: Solid Earth, 122(1), 572-591.

Gahalaut, V. K., Nagarajan, B., Catherine, J. K., & Kumar, S. (2006). Constraints on 2004 Sumatra–Andaman earthquake rupture from GPS measurements in Andaman–Nicobar Islands. Earth and Planetary Science Letters, 242(3-4), 365-374.

Heimann, S., Isken, M., Kühn, D., Sudhaus, H., Steinberg, A., Daout, S., ... & Dahm, T. (2018). Grond: A probabilistic earthquake source inversion framework.

Hurukawa, N., Wulandari, B. R., & Kasahara, M. (2014). Earthquake history of the Sumatran fault, Indonesia, since 1892, derived from relocation of large earthquakes. Bulletin of the Seismological Society of America, 104(4), 1750-1762.

Irwandi, I., Muksin, U., & Simanjuntak, A. V. (2021). Probabilistic seismic hazard map analysis for Aceh Tenggara district and microzonation for Kutacane city. In IOP Conference Series: Earth and Environmental Science (Vol. 630, No. 1, p. 012001). IOP Publishing.

McCaffrey, R. (2009). The tectonic framework of the Sumatran subduction zone. Annual Review of Earth and Planetary Sciences, 37, 345-366.

Muksin, U., Arifullah, A., Simanjuntak, A. V., Asra, N., Muzli, M., Wei, S., ... & Okubo, M. (2023). Secondary fault system in Northern Sumatra, evidenced by recent seismicity and geomorphic structure. Journal of Asian Earth Sciences, 105557.

Muksin, U., Bauer, K., & Haberland, C. (2013). Seismic Vp and Vp/Vs structure of the geothermal area around Tarutung (North Sumatra, Indonesia) derived from local earthquake tomography. Journal of volcanology and geothermal research, 260, 27-42.

Muksin, U., Haberland, C., Nukman, M., Bauer, K., & Weber, M. (2014). Detailed fault structure of the Tarutung Pull-Apart Basin in Sumatra, Indonesia, derived from local earthquake data. Journal of Asian Earth Sciences, 96, 123-131.

Nurana, I., Simanjuntak, A. V. H., Umar, M., Kuncoro, D. C., Syamsidik, S., & Asnawi, Y. (2021). Spatial Temporal Condition of Recent Seismicity In The Northern Part of Sumatra. Elkawnie: Journal of Islamic Science and Technology, 7(1), 131-145.

Pasari, S., Simanjuntak, A. V., Mehta, A., Neha, & Sharma, Y. (2021). A synoptic view of the natural time distribution and contemporary earthquake hazards in Sumatra, Indonesia. Natural Hazards, 108, 309-321.

Pasari, S., Simanjuntak, A. V., Mehta, A., Neha, & Sharma, Y. (2021). The current state of earthquake potential on Java Island, Indonesia. Pure and Applied Geophysics, 178, 2789-2806.

Pasari, S., Simanjuntak, A. V., Neha, & Sharma, Y. (2021). Nowcasting earthquakes in Sulawesi island, Indonesia. Geoscience Letters, 8, 1-13.

Sieh, K., & Natawidjaja, D. (2000). Neotectonics of the Sumatran fault, Indonesia. Journal of Geophysical Research: Solid Earth, 105(B12), 28295-28326.

Simanjuntak, A. V., & Ansari, K. (2022). Seismicity clustering of sequence phenomena in the active tectonic system of backthrust Lombok preceding the sequence 2018 earthquakes. Arabian Journal of Geosciences, 15(23), 1730.

Simanjuntak, A. V., Kuncoro, D. C., Irwandi, I., & Muksin, U. (2022). Understanding swarm earthquakes in Southeast Aceh, Sumatra. In E3S Web of Conferences (Vol. 339, p. 02011). EDP Sciences.

Simanjuntak, A., Muksin, U., Asnawi, Y., Rizal, S., & Wei, S. (2022). Recent Seismicity and Slab Gap Beneath Toba Caldera (Sumatra) Revealed Using Hypocenter Relocation Methodology. Geomate Journal, 23(99), 82-89.

Waldhauser, F. (2001). HYPODD--A program to compute double-difference hypocenter locations, U.S. Geologic Survey Open-File Report.

Waldhauser, F. and W.L. Ellsworth (2000). A double-difference earthquake location algorithm: Method and application to the Hayward fault, Bulletin of the Seismological Society of America 90, 1353-1368.